Journal of Cosmology and
Astroparticle Physics

Revisiting the axion bounds from the Galactic white dwarf luminosity function

To cite this article: M.M. Miller Bertolami *et al* JCAP10(2014)069

Journal of Cosmology and Astroparticle Physics
An IOP and SISSA journal

Revisiting the axion bounds from the Galactic white dwarf luminosity function

M.M. Miller Bertolami,[a,b,1,2] **B.E. Melendez,**[b,c] **L.G. Althaus**[b,c] **and J. Isern**[d,e]

[a]Max-Planck-Institut für Astrophysik,
Karl-Schwarzschild-Str. 1, 85748, Garching, Germany
[b]Instituto de Astrofísica de La Plata, UNLP-CONICET,
Paseo del Bosque s/n, 1900 La Plata, Argentina
[c]Grupo de evolución estelar y pulsaciones, Facultad de Ciencias Astronómicas y Geofísicas,
Universidad Nacional de La Plata, Paseo del Bosque s/n, 1900 La Plata, Argentina
[d]Institut de Ciéncies de l'Espai (CSIC),
Facultat de Ciéncies, Campus UAB, Torre C5-parell, 08193 Bellaterra, Spain
[e]Institute for Space Studies of Catalonia,
c/Gran Capitá 2-4, Edif. Nexus 104, 08034 Barcelona, Spain.

E-mail: marcelo@MPA-Garching.MPG.DE, brenmele@gmail.com,
althaus@fcaglp.fcaglp.unlp.edu.ar, isern@ieec.cat

Received July 1, 2014
Revised September 23, 2014
Accepted October 7, 2014
Published October 27, 2014

Abstract. It has been shown that the shape of the luminosity function of white dwarfs (WDLF) is a powerful tool to check for the possible existence of DFSZ-axions, a proposed but not yet detected type of weakly interacting particles. With the aim of deriving new constraints on the axion mass, we compute in this paper new theoretical WDLFs on the basis of WD evolving models that incorporate the feedback of axions on the thermal structure of the white dwarf. We find that the impact of the axion emission into the neutrino emission can not be neglected at high luminosities ($M_{\rm Bol} \lesssim 8$) and that the axion emission needs to be incorporated self-consistently into the evolution of the white dwarfs when dealing with axion masses larger than $m_a \cos^2\beta \gtrsim 5$ meV (i.e. axion-electron coupling constant $g_{ae} \gtrsim 1.4\times10^{-13}$). We went beyond previous works by including 5 different derivations of the WDLF in our analysis. Then we have performed χ^2-tests to have a quantitative measure of the agreement between the theoretical WDLFs — computed under the assumptions of different

[1]Corresponding author.
[2]On leave of absence from CONICET.

doi:10.1088/1475-7516/2014/10/069

JCAP10(2014)069

axion masses and normalization methods — and the observed WDLFs of the Galactic disk. While all the WDLF studied in this work disfavour axion masses in the range suggested by asteroseismology ($m_a \cos^2\beta \gtrsim 10$ meV; $g_{ae} \gtrsim 2.8 \times 10^{-13}$) lower axion masses can not be discarded from our current knowledge of the WDLF of the Galactic Disk. A larger set of completely independent derivations of the WDLF of the galactic disk as well as a detailed study of the uncertainties of the theoretical WDLFs is needed before quantitative constraints on the axion-electron coupling constant can be made.

Keywords: axions, white and brown dwarfs, stars, dark matter detectors

ArXiv ePrint: 1406.7712

Contents

1 Introduction

Despite its success, the standard model of particle physics has some unsolved issues. Among them, is the CP-problem of Quantum Chromodynamics (QCD), i.e. the absence of a CP-violation in the strong interactions. One elegant solution to the CP-problem is the Peccei-Quinn mechanism [1] in which the coefficient of the CP-violating term of the QCD lagrangian is proposed to be a dynamical field (the *axion field*) whose vacuum expectation value naturally leads to CP-conservation. One of the natural consequences of such mechanism is the existence of a new particle, the *axion* [2, 3]. Soon after its proposal it was realized that stellar astrophysics was an excellent tool to constrain axion properties [4]. While the original axion models were soon ruled out by observations, "invisible" axion models such as the DFSZ [5, 6] and KSVZ models [7, 8] are much more elusive (see [9] for a review). In particular DFSZ-type axions couple to electrons and would be emitted from the interior of white dwarfs (WD) and red giant cores, opening the possibility of using those stellar populations as laboratories to constrain axion properties (e.g. [10–12], and more recently [13]). The coupling strength between electrons and DFSZ-axions is defined by the axion-electron adimensional coupling constant, g_{ae}, which is related to the mass of the axion (m_a) through

$$g_{ae} = 2.8 \times 10^{-14} \times m_{a[\rm meV]} \times \cos^2\beta \tag{1.1}$$

where $\cos^2\beta$ is a model dependent parameter. g_{ae} is also related to the axionic fine structure constant α_{26} by

$$\alpha_{26} = 10^{26} \times {g_{ae}}^2/4\pi. \tag{1.2}$$

Because the evolution of white dwarfs is mostly a simple cooling process and the basic physical ingredients needed to predict their evolution are relatively well known, white dwarfs offer a unique opportunity to test new physics under conditions that can not be obtained in present day laboratories [14–16]. In the last decade, the white dwarf luminosity function (WDLF) has been noticeably improved by large sky surveys [17–20], leading to the possibility of new studies of the impact of the axion emission in the WDLF. Based on these improvements of the WDLF [12, 21] computed the impact of the axion emission in the WDLF by adopting a perturbative approach on the axion emission. [12, 22] find that the inclusion of the DFSZ-axion emissivity, with $m_a \cos^2\beta \sim 5$ meV, in the evolutionary models of white dwarfs would improve the agreement between the theoretical and observational WDLFs, and that axion masses $m_a \cos^2\beta > 10$ meV are clearly excluded. Interestingly enough, these values were in concordance with the values obtained from the secular drift of the period of pulsation of ZZ Ceti stars [11, 23, 24]. However, the recent analysis of the observed pulsation period of G117-B15A and R548 have provided a value of $m_a \cos^2\beta = 17.4^{+2.3}_{-2.7}$ meV and $m_a \cos^2\beta = 17.4^{+4.3}_{-5.8}$ meV respectively [25, 26]. Interestingly enough, based on an older determination of the observed period drift [27] and simplified chemical profiles, a similar result (10.4 meV$\lesssim m_a \cos^2\beta \lesssim 26.5$ meV) was suggested by the thick envelope solutions of [24]. It should be noted that for axion masses as high as $m_a \cos^2\beta \sim 17$ meV the axion emission becomes the dominant cooling process down to very low luminosities ($M_{\rm Bol} \sim 13$). In such a situation, we expect the existence of a significant axion emission to impact the thermal structure of the white dwarf. Thus, for the range of interest of the axion masses suggested by asteroseismology the axion emission can not be treated as a perturbation to the white dwarf cooling and a self consistent treatment of the axion emission is necessary. In view of the previous arguments, the inconsistency between the masses derived by both methods calls for a reanalysis of the previous results in the light of a self consistent treatment of the axion emission. In addition, new determinations of the WDLF that extend to the high luminosity regime have become recently available [19, 20]. At these luminosities the axion emission can be very important even for low axion masses. Hence, to make use of the new available data, full evolutionary models derived from the progenitor history are also needed.

In the present work, we analyze constraints on the axion mass by means of a detailed analysis of the WDLF of the Galactic disk. We go beyond previous works by studying the impact of the axion emission in the cooling of white dwarfs by means of a self consistent treatment of the axion emission and state of the art white dwarf models. In addition, we extend the scope of our work by taking into account different derivations of the Galactic WDLF. In particular, we include in the analysis an estimation of the WDLF of bright white dwarfs. Also, we analyze to which extent the normalization procedure adopted for the white dwarf luminosity function affect the results. The paper is organized as follows: in the next section we describe the numerical tools, input physics and initial white dwarf models. We also describe briefly the method adopted to compute the theoretical white dwarf luminosity functions. In section 3, we present the results of the impact of the axion emission in the white dwarf models, paying special attention to the feedback of the axion emission in the thermal structure of the white dwarf. Next, in section 4 we quantitatively assess the impact of the axion emission in the theoretical WDLF and compare with different empirical WDLFs. Finally, in section 5 we summarize our results and conclusions and propose some future work that needs to be done in order to improve these constrains.

2 Numerical tools

2.1 Input physics and initial white dwarf models

The stellar evolution computations presented in this work have been performed with `LPCODE` stellar evolution code, which has been used to study different problems related to the formation and evolution of white dwarfs — e.g. [28–30]. A detailed description of the code is available in [29] and references therein, here we only mention those which are most relevant

JCAP10(2014)069

for the present work. The main physical ingredients included in the simulations of white dwarfs computed with LPCODE comprise the following. The equation of state for the high density regime is that of [31] while for the low density regime we use an updated version of the equation of state of [32] (Mazzitelli 1993, private communication). Conductive opacities are those of [33] while radiative opacities are those of the OPAL project [34] complemented at low temperatures by the molecular opacities produced by [35]. White dwarf models computed with LPCODE also include detailed non-gray model atmospheres to provide accurate boundary conditions for our models which include non-ideal effects in the gas equation of state, see [36] for details. Neutrino cooling by Bremsstrahlung, photo and pair production are included following the recipes of [37], while plasma processes are included according to [38]. All relevant energy sources are taken into account in the simulations, including marginal nuclear burning, the release of latent heat and the gravitational energy associated with the phase separation in the carbon-oxygen profile induced by crystallization. The inclusion of all these energy sources is done self-consistently and locally coupled to the full set of equations of stellar evolution. In addition the effects of time dependent element diffusion during the white dwarf evolution is also taken into account following treatment of [39] for multicomponent gases. It is worth noting for the aim of the present work that LPCODE has recently been tested against other well-known stellar evolution code and it was found that uncertainties in white dwarf cooling times arising from different numerical implementations of the stellar evolution equations were below 2% [40]. This, together with the state of the art input physics adopted in LPCODE provides a very solid ground for the present work.

The initial white dwarf models adopted in our simulations were taken from [41] and [29]. Specifically 4 different initial white dwarf models of $0.524 M_\odot$, $0.609 M_\odot$, $0.705 M_\odot$ and $0.877\ M_\odot$ were adopted. These models were obtained from computing the complete evolution of initially $1 M_\odot$, $2 M_\odot$, $3 M_\odot$ and $5\ M_\odot$ ZAMS stars with Z=0.01, which is in agreement with semi-empirical determinations of the initial-final mass relationship [42]. Note that physically sounding initial WD models are relevant at relatively high luminosities. In fact, [40] found that, at $\log L/L_\odot \gtrsim -1.5$, differences up to 8% can be found due to gravothermal differences in the initial white dwarf models, even when the same chemical stratification is adopted.

2.2 DFSZ-axion emission

For the sake of completeness DFSZ-type axion emission by both Compton and Bremsstrahlung processes were included in LPCODE, although only Bremsstrahlung processes are relevant in white dwarfs. Also, expressions concerning the axion emissivity were included for both the strong ($\Gamma > 1$)[1] and weak ($\Gamma < 1$) ion-correlations and for both the strongly degenerate and non-degenerate regimes. In what follows, for the sake of clarity, we describe the adopted expression for DFSZ-axion emissivity. Axion Bremsstrahlung emission under degenerate conditions ($\epsilon_{\rm BD}$) was included adopting the prescriptions of [43, 44] for strongly coupled plasma regime ($\Gamma > 1$)

[1]Where the ionic coupling constant Γ for multicomponent plasmas is defined following [31] as

$$\Gamma = 2.275 \times 10^5 \frac{(\rho Y_e)^{1/3}}{T} \sum_i (n_i/n_{\rm ions}) Z_i{}^{5/3},$$

where the sum is taken over all considered nuclear species.

and [45] for weakly coupled plasmas ($\Gamma < 1$). Specifically, we computed

$$\epsilon_{\rm BD} = 10.85\ \alpha_{26}\ {T_8}^4 \sum_j^{N_{\rm isot}} \frac{X_j {Z_j}^2}{A_j} \times F_j \tag{2.1}$$

were F_j is given by [43, 44] for $\Gamma > 1$ and in the case of $\Gamma < 1$ is given by $F_j = F$ where

$$\begin{aligned} F =\ & \frac{2}{3}\ln\left(\frac{2+\kappa^2}{\kappa^2}\right) \\ & + \left[\frac{2+5\kappa^2}{15}\ln\left(\frac{2+\kappa^2}{\kappa^2}\right) - \frac{2}{3}\right] \times {\beta_F}^2 \end{aligned} \tag{2.2}$$

with β_F and κ given as

$$\kappa^2 = \frac{2\pi\alpha\hbar^3 c}{m_u k}\frac{\rho}{T}\sum_j \frac{X_j {Z_j}^2}{A_j}\frac{1}{{p_F}^2}, \tag{2.3}$$

$${\beta_F}^2 = \frac{{p_F}^2}{{m_e}^2 c^2 + {p_F}^2}, {p_F}^2 = \hbar\left(\frac{3\pi^2\rho}{\mu_e m_u}\right)^{1/3}. \tag{2.4}$$

For the non-degenerate regime ($\epsilon_{\rm BND}$), Bremsstrahlung was derived from the expressions presented in [9], specifically we adopted

$$\begin{aligned} \epsilon_{\rm BND} =\ & 5.924 \times 10^{-4}\ \alpha_{26} \frac{{T_8}^{5/2}\rho}{\mu_e} \sum_{j=1}^{N_{\rm isot}} \left[\frac{X_j}{A_j}\right] \\ & \times \left[{Z_j}^2\left(1 - \frac{5}{8}\frac{\kappa^2\hbar^2}{m_e T k}\right) \frac{Z_j}{\sqrt{2}}\left(1 - \frac{5}{4}\frac{\kappa^2\hbar^2}{m_e T k}\right)\right]\ \left[\frac{\rm erg}{\rm g\ s}\right]. \end{aligned} \tag{2.5}$$

with the screening scale κ computed as

$$\kappa^2 = \frac{4\pi\alpha\hbar c}{kT}\hat{n}, \quad \hat{n} \simeq n_e + \sum_j^{N_{\rm isot}} {Z_j}^2 n_j. \tag{2.6}$$

Axion emission by Compton processes was included following [45] taking into account the effects of Pauli blocking under degenerate conditions and relativistic corrections,

$$\epsilon_{\rm compton} = 33\ \alpha_{26}\ Y_e\ {T_8}^6\ F_c \quad {\rm erg\ g^{-1}\ s^{-1}}. \tag{2.7}$$

Where, following [45], we computed F_c as

$$F_c = \left(1 + {F_{\rm comp.deg.}}^{-2}\right)^{-1/2}. \tag{2.8}$$

with

$$F_{\rm comp.deg.} = 4.96 \times 10^{-6} {\mu_e}^{2/3} \frac{T}{\rho^{2/3}}. \tag{2.9}$$

Then, the total axion emission ($\epsilon_{\rm axion}$) was then computed as:

$$\epsilon_{\rm axion} = \epsilon_{\rm Brem} + \epsilon_{\rm compton} \tag{2.10}$$

where the Bremsstrahlung emission was obtained from

$$\epsilon_{\rm Brem} = \left(\frac{1}{\epsilon_{\rm BND}} + \frac{1}{\epsilon_{\rm BD}}\right)^{-1} \tag{2.11}$$

$\epsilon_{\rm BD}$ was then computed as $\epsilon_{\rm BD\,(\Gamma<1)}$ if $\Gamma < 0.9$, $\epsilon_{\rm BD\,(\Gamma>1)}$ if $\Gamma > 1.1$ and interpolated linearly between both expressions when $\Gamma \in (0.9, 1.1)$. It is worth noting that, while the details of the interpolation scheme will significantly affect the axion emission in intermediate regimes the mass of those regions is small and will not introduce any significant change in the global cooling speed of the white dwarf.

2.3 Theoretical white dwarf luminosity functions

As mentioned in the introduction, with the current knowledge of the WDLF it is possible to put constraints on the axion mass independently from those coming from asteroseismoogy. In particular, as the WDLF reflects the global properties of the whole population of white dwarfs we expect it to be less sensitive to the accuracy of our understanding of the internal structure of individual white dwarf stars, as it is the case in asteroseismological determinations of the axion mass. Of course, this advantage is obtained at the price of relying on our present knowledge of stellar population properties such as initial mass functions (IMF) and galactic stellar formation rates (SFR) which do not play any role in asteroseismological determinations. Fortunately, as shown by [12], the details of those ingredients do not seem to play an important role if the range of WD luminosities used for WDLF comparisons is appropriately chosen.

To construct theoretical white dwarf luminosity functions we adopted the method presented by [46]. Thus, the number of white dwarfs per logarithmic luminosity and volume is computed as

$$\frac{dn}{dl} = -\int_{M_1}^{M_2} \psi(t) \left(\frac{dN}{dM}\right) \left(\frac{\partial t_c}{\partial l}\right)_m dM \tag{2.12}$$

where $\psi(t)$ is the galactic stellar formation rate at time t, $N(M)$ is the initial mass function and $t_c(l,m)$ is the time since the formation of a white dwarf, of mass m, for the star to reach a luminosity $log(L/L_\odot) = l$. In order to compute the integral in equation (2.12) we also need the initial-final mass relation $m(M)$, and the pre-white dwarf stellar lifetime $t_{ev}(M)$. It is worth noting that, for a given white dwarf luminosity (l) and mass of the progenitor (M) the formation time of the star, t, is obtained by solving

$$t + t_{ev}(M) + t_c(l,m) = T_{OS}, \tag{2.13}$$

where T_{OS} is the assumed age of the oldest star in the computed population. The lowest initial mass that produces a white dwarf with luminosity l at the present time (M_1) is obtained from eq. (2.13) when $t = 0$. The value of M_2 corresponds to the largest stellar mass progenitor that produces a white dwarf.

In order to compute the impact of axions on the white dwarf luminosity function, for each initial white dwarf model, 8 cooling sequences with different assumed axion masses were computed ($m_a \cos^2\beta$= 0, 2.5, 5, 7.5, 10, 15, 20 & 30 meV). In addition, to compute eq. (2.12) we adopt a Salpeter initial mass function, the initial-final mass relation from [42], the stellar lifetimes from the BaSTI database [47] and constant star formation rate.

As shown by [12] the bright part of the WDLF is almost independent of the stellar formation rate or the age of the disk, as their main effects are absorbed in the normalization procedure. For the sake of comparison with [12] for most of the computations we compared the theoretical and observationally derived WDLF within the range $-1 \leq log(L/L_\odot) \leq -3$ ($7.25 \leq M_{\rm Bol} \leq 12.25$)[2]. A disk age of 11 Gyr is assumed throughout the present work ($T_{OS} = 11$ Gyr). Regarding the normalization of the theoretical WDLF we tried two different approaches. First we followed [12] and normalized the WDLF so that, for a given $l_{\rm bin}$ value we have

$$\frac{dn}{dl}(l_{\rm bin}) = n^{\rm O}(l_{\rm bin}) \tag{2.14}$$

where $n^{\rm O}(l_{\rm bin})$ stands for the number of stars per volume, per luminosity bin, inferred in Galactic WDLFs [12, 17, 18] in the luminosity bin with $log(L/L_\odot) = l_{\rm bin}$. This was done taking $l_{\rm bin}$ equal to all luminosity bins presented between $l \simeq -2$ and $l \simeq -3$ (the exact value depending on the binning of each WDLF). Only normalization points in the low luminosity range should be preferred. Otherwise, axions are a dominant cooling mechanism at the normalization luminosity and the differential effect of the axion emission is hidden. As will be seen in section 4, the choice of the specific normalization point does not affect the main conclusion of the work, but it has some impact in the quantitative comparison between theoretical and observationally derived WDLF. In order to make the theoretical WDLF less dependent on the particular normalization point we also adopted a second normalization scheme. Specifically, we normalized the WDLF by requiring the total number of stars per volume in a given magnitude range $(M^1_{\rm Bol}, M^2_{\rm Bol})$ to fit the observations , i.e.

$$\sum_{M^i_{\rm Bol} \in (M^1_{\rm Bol}, M^2_{\rm Bol})} n^{\rm O}(M^i_{\rm Bol}) \Delta M_{\rm Bol} = \int_{M^1_{\rm Bol}}^{M^2_{\rm Bol}} \frac{dn}{dl} dM_{\rm Bol}. \tag{2.15}$$

Our preferred choice is $M^1_{\rm Bol} = 9.5$ (9.6) and $M^2_{\rm Bol} = 12.5$ (12.4) for [12, 17, 20] and [48] [18] WDLFs.

3 Impact of axion emission in white dwarf cooling

Figure 1 shows the axion, photon and neutrino emission for a white dwarf of $0.609 M_\odot$ under the assumption of different axion masses. It is clear from figure 1 that axion emission leads to a decrease of the neutrino emission at the same WD luminosity. One of the results of our computations is the realization that the feedback of the axion emission into the neutrino emission can not be neglected in the range of axion masses suggested by asteroseismological determinations ($m_a > 10$ meV, [25, 26]) at relatively high WD luminosities ($M_{\rm bol} \lesssim 8$). This result is due to the fact that when axion emission is included this leads to an extra cooling of the white dwarf core which alters the thermal structure of the white dwarf, as compared with the case without axion emission. This, in turn, leads to a decrease of the neutrino emission at a given surface luminosity of the star. The main consequence of this is that WD cooling is less sensitive to the existence of axions, than a perturbative approach would suggest, due to the additional energy loss due to the existence of axions is then counterbalanced by the decrease of the energy lost by neutrino emission. Note that for axion masses as small as $m_a \cos^2\beta = 5$ meV the neutrino emission is already affected by the axion emission, being different from the case with no axions ($m_a \cos^2\beta = 0$ meV). Consequently the axion emission needs to be treated self-consistently for high luminosity WDs ($M_{\rm bol} \lesssim 8$) when dealing with axions

[2] Throughout this work the assumed relationship between the bolometric magnitude and the luminosity of the star is adopted consistently with the data of [17] (i.e. $M_{\rm Bol} = -2.5 \log(L/L_\odot) + 4.75$).

JCAP10(2014)069

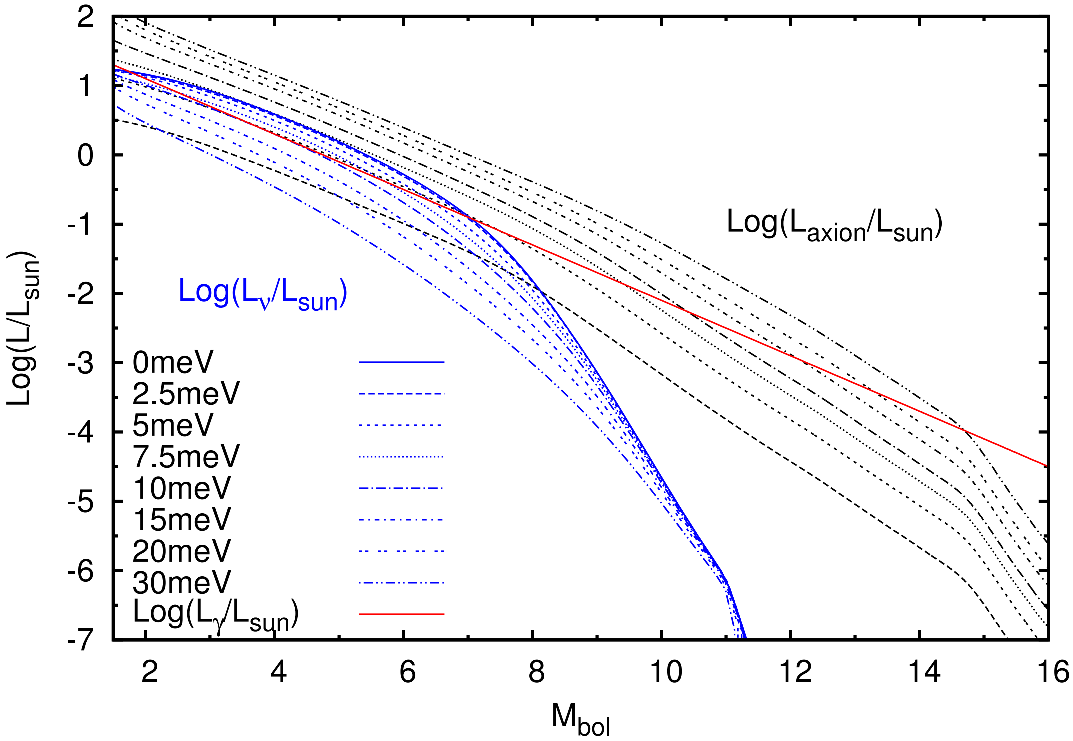

Figure 1. Axion (black curves) and neutrino (blue curves) emission for our $0.609M_\odot$ sequences for different axion masses. The impact of the axion emission in the thermal structure of the white dwarf can be appreciated in the decrease of the neutrino emission at higher axion masses. Clearly, axion emission can not be treated perturbatively at $m_a \cos^2\beta > 5$meV.

in the range claimed by asteroseismology or detectable through the white dwarf luminosity function. At lower luminosities ($M_{\rm bol} \gtrsim 8$) the neutrino emission becomes negligible and thus the cooling speed is unaffected by the feedback of axion emission. Clearly, at low luminosities the feedback of axion emission into the total energy loss of the star is negligible.

In figure 2 the axion and neutrino emission of our $0.609M_\odot$ sequence is compared with the $0.61M_\odot$ sequence of [12] for an axion of $m_a \cos^2\beta = 5$ meV. There is an overall good agreement for axion emission between both predictions at low luminosities ($M_{\rm bol} \gtrsim 7$). The departure between both curves at high luminosities ($M_{\rm bol} \lesssim 7$) can be traced back to the isothermal core approximation of [12] which leads to an underestimation of the axion emission at high luminosities when the maximum temperature of the core is located off-centered. Also, as mentioned before, to obtain accurate cooling timescales the feedback of the axion emission into the thermal structure of the white dwarf is only relevant for high luminosity WDs ($M_{\rm bol} \lesssim 8$) and thus, only marginally relevant for the range of luminosities studied in most of the present work ($7 \leq M_{\rm Bol} \leq 12.5$). Consequently, for the aim of comparing theoretical and observed WDLFs in the range $7 \leq M_{\rm Bol} \leq 12.5$ the impact of the approximations adopted by [21] and [12] are not significant.

4 Impact of the axion emission in the WDLF

In order to take into account possible systematics in the comparison and also to allow for a direct comparison with previous works, we have adopted five different derivations of the

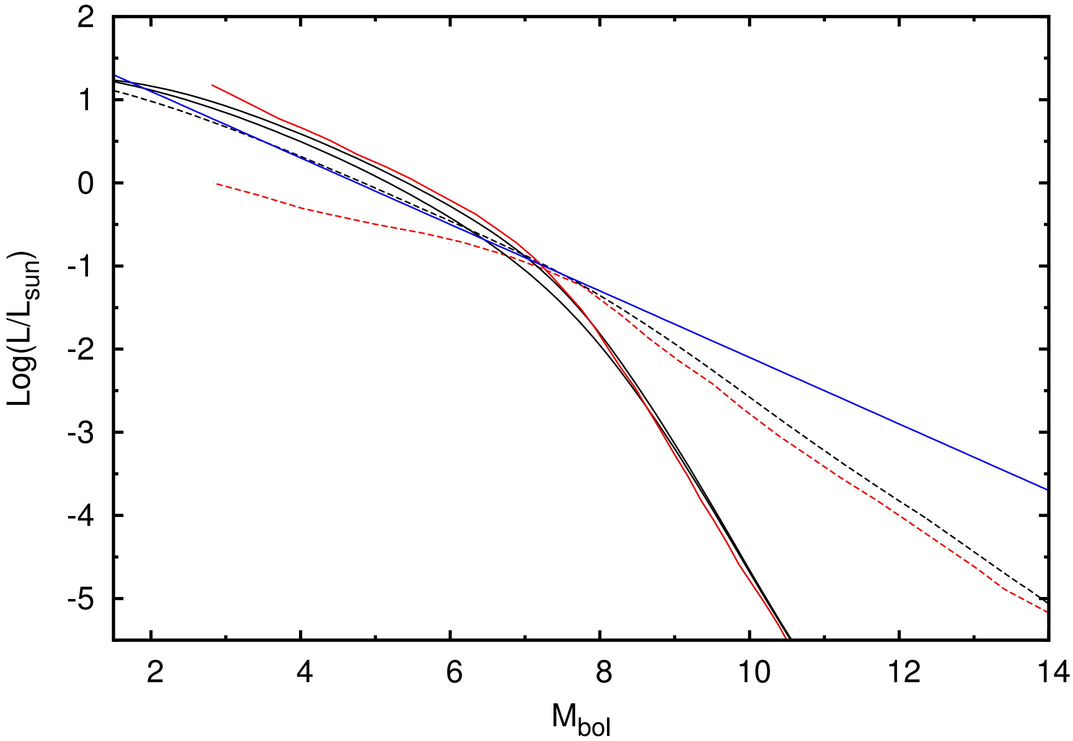

Figure 2. Comparison of the axion ($m_a \cos^2 \beta = 5$meV) and neutrino emission of our $0.609 M_{\odot}$ and the $0.61 M_{\odot}$ sequence of [12]. The black solid lines represent the neutrino luminosity (from top to bottom: $m_a \cos^2 \beta = 0$, 5meV) for our model. The red solid line represents the neutrino emission of Isern model. The black dashed line represents the 5meV axion emission for our model and the red dashed line represents the 5meV axion emission of [12] model. The blue solid line represents the photon luminosity. The effects of the departure from the isothermal core approximation can be appreciated at $M_{\rm bol} < 7$.

WDLF of the Galatic disk. Specifically, we compare our theoretical WDLFs with those derived, or constructed, by [12, 17, 18, 20, 48], see figure 3. While the WDLF of [17] was derived from the SDSS-DR3 using the reduced proper motion technique without separeating them into H-rich and H-deficient white dwarfs, the WDLF of [18] was derived from the SDSS-DR4 but constraing it to spectroscopically identified H-rich white dwarfs. In order to allow for a direct comparison of our results with those presented by [12], we have also included in our study the WDLF presented by [12].[3] All the previous WDLF come from the SDSS survey so we also included in our analysis the, completely independent, WDLF derived by [20] from the SuperCOSMOS Sky Survey. Finally, to make full use of the new WDLFs that extend to the high luminosity regime, we have also included the WDLF constructed by [48] from two sets of completely independent WDLFs [19, 20].

4.1 WDLFs at intermediate luminosities

In figure 4 we show, as an example, the resulting white dwarf luminosity functions for each axion mass as compared with the WDLF derived by [17]. It can be clearly seen that axion

[3] This WDLF was constructed from the DR3-SDSS data (Harris, March 2005, private communication) with $V_{\rm tan} > 20$ km/s.

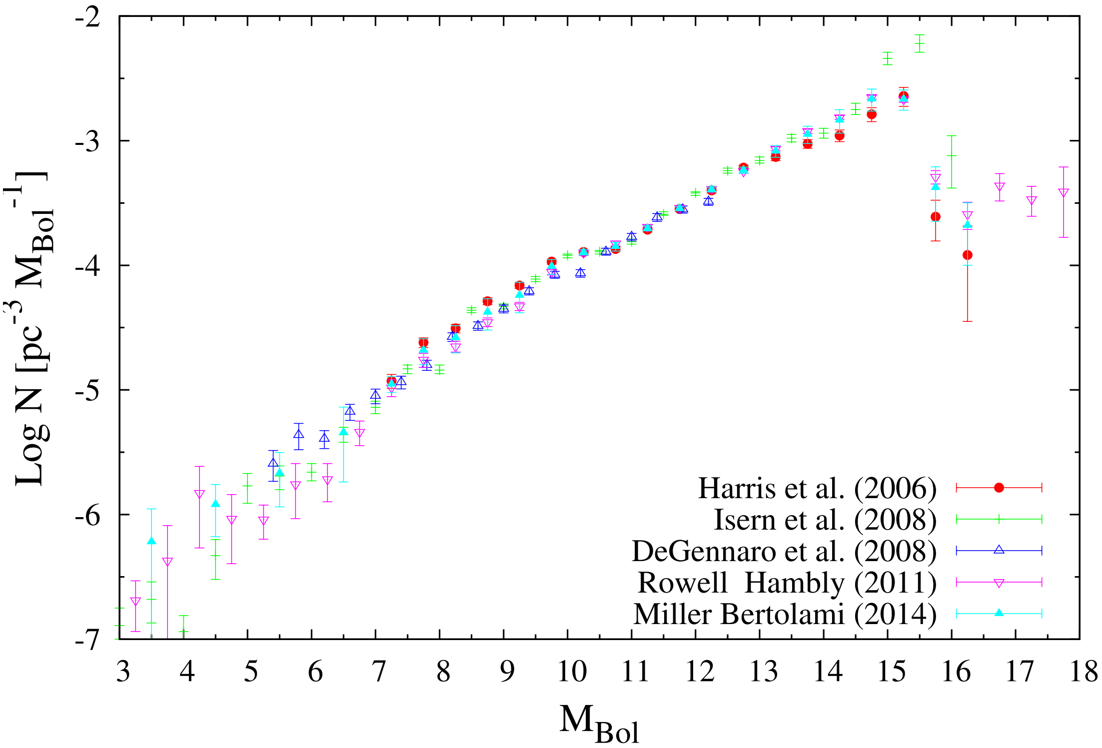

Figure 3. White Dwarf luminosity functions of the Galactic disk adopted for comparison in this work. In this plot the WDLF from [20] has been multiplied by a factor of 1.862 as described in [48].

masses larger than 10 meV would lead to apparent disagreements with the luminosity function derived by [17]. Large axion masses are also in disagreement with the WDLFs of [12, 18] and [20]. To have a quantitative measure of the agreement between the WDLF computed under different assumptions and the observational WDLFs (figure 3), we have performed a χ^2-test. The value of χ^2 was computed as

$$\chi^2(m_a) = \frac{1}{(N-1)} \sum_{i=1}^{N} \frac{(n_i^{\rm O} - n_i^{m_a})^2}{{\sigma_i}^2}, \tag{4.1}$$

where $N = 11$ [17, 20], 13 [18] or 10 [12], $n_i^{\rm O}$ stands for the values derived in each observational WDLF and $n_i^{m_a}$ is the theoretically computed number of stars under the assumption of different axion masses (m_a). We have estimated σ_i as those presented in each observational WDLF, which means that we are neglecting errors coming from the uncertainties in the theory of stellar evolution. The $N-1$ in eq. (4.1) takes into account the fact that the $n_i^{m_a}$ values are not completely independent of the observations, as they are normalized to fit the observations, as described in eqs. (2.14) and (2.15).

The χ^2-values obtained from eq. (4.1) are, in all the cases, too large, according to χ^2- test, implying that a significant disagreement exists between all the derived theoretical WDLFs and the observations. The reasons for this disagreement seems to be two-folded. On the one hand the different WDLFs are not consistent between themselves, suggesting that the uncertainties are larger than quoted in the WDLFs. On the other hand, our method does not quantify the uncertainties in the constructed WDLFs. In particular, very recent

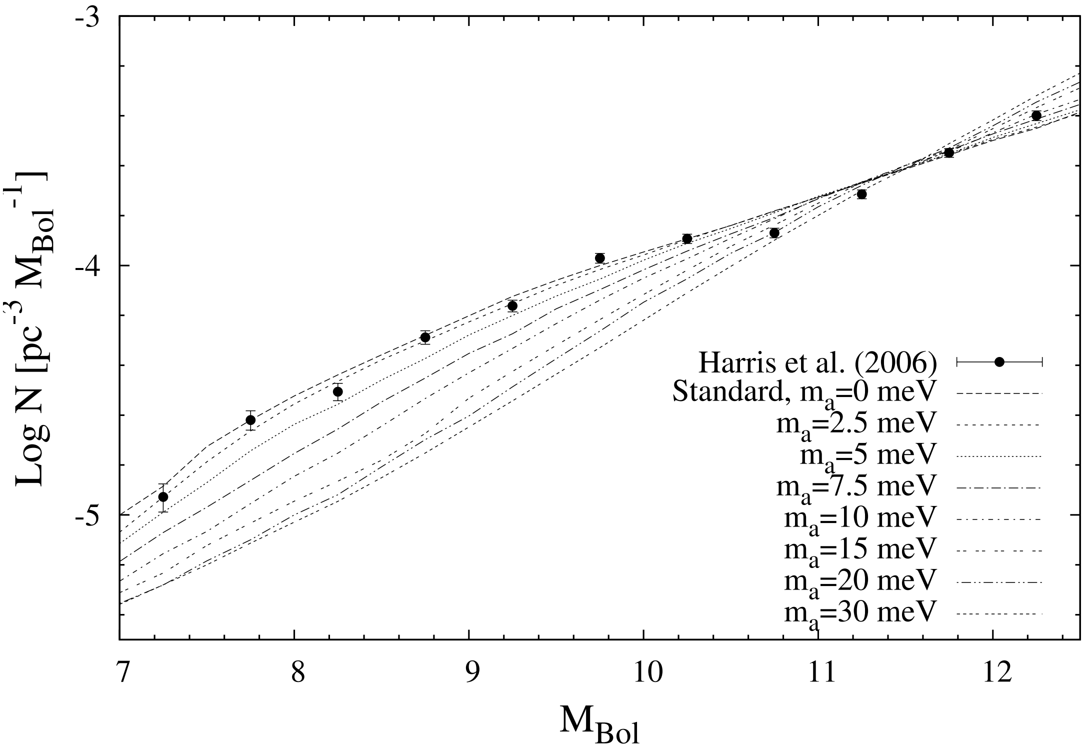

Figure 4. White Dwarf luminosity function constructed for the different axion masses compared with the luminosity function derived by [17]. DFSZ-axions heavier than $m_a > 10$meV are clearly excluded by the observed white dwarf luminosity functions. Note that theoretical WDLF constructed with $m_a \geq 10$meV almost overlap each other in the range of interest. This is due to the fact that the normalization region is, then, also affected by the axion emission.

short term fluctuations in the late SFR of the Galaxy might introduce sizeable departures from the assumption of a constant SFR. Fortunately, although the derived χ^2-values are large, significant differences of more than one order of magnitude exist between the best-fit χ^2-values and the rest.

In figure 5 we show the χ^2-values relative to the best fit value for each normalization point and for each WDLF. As apparent from figure 5, while the WDLF of [17] points towards values of the axion mass $m_a \cos^2\beta \lesssim 2.5$ meV the WDLFs from [18] and [20] favour the existence of some extracooling implying axion masses of 5 meV$\lesssim m_a \cos^2\beta \lesssim 7.5$ meV. It is particulartly worth noting that the essence of this result is true independent of the normalization point, or normalization method, of the theoretical WDLF. In fact, when we adopt the second normalization method for the WDLF (eq. (2.15)) we reobtain the same global result. The different favoured axion mass value should not be surprising, as it is apparent from figure 3 that the differences between WDLFs are beyond the quoted error bars. In addition, when we compare with the WDLF adopted by [12] (which is a preliminar version of that in [17]) we reobtain the main results quoted in that article, that the best fit models imply values of the axion mass in the range 2.5 meV$\lesssim m_a \cos^2\beta \lesssim 7.5$ meV, depeding on the normalization point/method. Note, however, that in this case differences in the χ^2-values are smaller than in the three previous cases and less stringent constraints can be drawn.

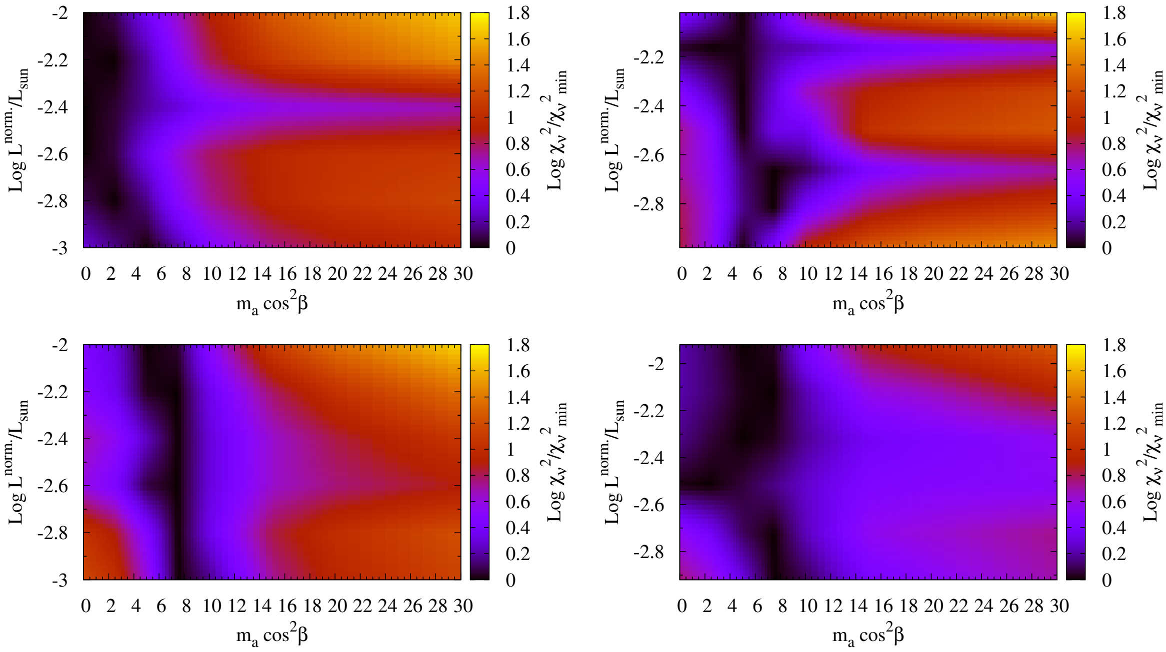

Figure 5. χ^2-values (color map) derived from the comparison of the theoretical WDLFs with those obtained by [17] (top left), [18] (top right), [20] (bottom left) and [12] (bottom right), for different choices of the normalization point (y-axis) and the mass of the axion (x-axis).

4.2 Constraints from the WDLF at $3 < M_{\rm Bol} < 12.5$

Figure 6 shows the comparison between the theoretical WDLF computed for different axion masses with the WDLF of the Galactic disk constructed by [48]. This WDLF was constructed from the WDLF determined by the SDSS [17, 19] and the SuperCOSMOS [20] sky surveys. The size of the error bars reflects the discrepancies between both WDLFs. Consequently, the error bars not only reflect internal statistical uncertainties but also systematic discrepancies between both WDLF — see [48] for a detailed discussion on these issues. In addition, this WDLF includes information from the WDLF at much higher luminosities where axions are expected to be an important cooling mechanism even for low axion masses. As in the previous cases we have compared the theoretical and observational WDLFs by adopting different normalization points and methods (eqs. (2.14) and (2.15)). As it happened in the previous cases (figure 5) for the first normalization method the best fit theoretical luminosity function depends slightly on the adopted normalization point, but the main result is stable: a χ^2-test marginally prefers values around $m_a \cos^2\beta \lesssim 5$ meV while axion masses of $m_a \cos^2\beta \gtrsim 10$ meV are excluded at a high significance level. This can be seen in figure 6 where the results in the case of the second normalization method are shown. As can be seen in the inset, while the best fit model corresponds to $m_a \cos^2\beta \lesssim 5$ meV all models below $m_a \cos^2\beta \lesssim 7.5$ meV can not be rejected at a 2σ-like confidence level. On the contrary, all theoretical WDLFs constructed with $m_a \cos^2\beta \gtrsim 10$ meV are strongly at variance with the WDLF from [48].

5 Discussion and conclusions

In order to place constraints on the possible coupling strength between axions and electrons (g_{ae}) we have performed a detailed study of the impact of the axion emission on the cooling

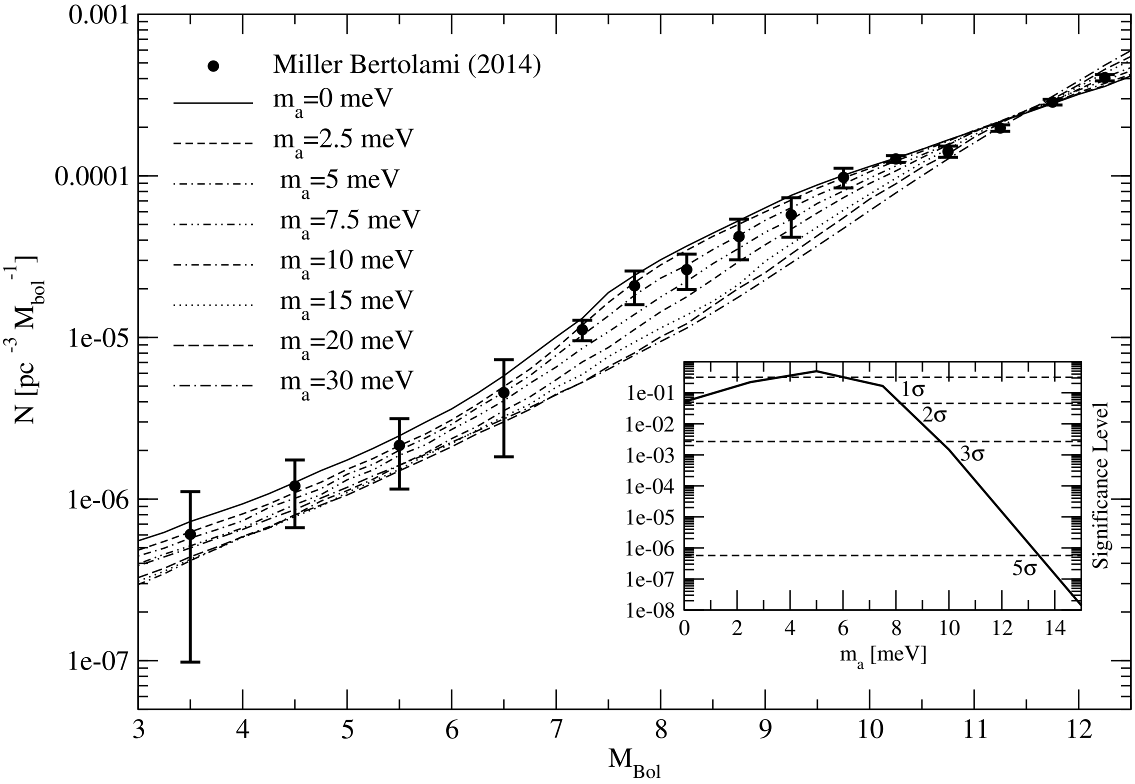

Figure 6. Comparison of the WDLF constructed by [48] with the theoretical WDLF for different axion masses. The continuous line in the inset shows the significance level at which different values of the axion mass are discarded by a χ^2-test. The significance levels associated with different σ-values are show for reference with short dashed lines.

of white dwarfs. In particular, we improved previous works by including a self consistent treatment of the axion emission into the thermal structure of the white dwarf models, and by including several different WDLFs in the analysis. In particular, for the first time we extended the comparison to the high luminosity regime where axions are expected to be the main cooling channel. This was performed on the basis of state of the art initial white dwarf models and microphysics. In addition, we tested the dependence of the comparison on the choice of the normalization points of the theoretical WDLFs, as well as on the normalization method adopted. We quantitatively weighted the agreement between theory and observations by means of a χ^2-fit.

The main results of the present work can be summarized as follows. In the luminosity range $7 \leq M_{\rm Bol} \leq 12.5$ we find an overall good agreement between the perturbative approach adopted by [12] and the result of the self-consistent full-evolutionary computations presented here. On the contrary, for the range $M_{\rm Bol} \leq 7$ both the feedback of the axion emission on the thermal structure of the white dwarf and the departure from the isothermal core approximation need to be taken into account. This is worth noting in the light of new determinations of the WDLF which extend to higher luminosities and temperatures. From an inspection of the results in figures 5 and 6 we can conclude that the values of $m_a \cos^2\beta \simeq 17$ meV inferred from the asteroseismology of G117-B15A and R548 [25, 26] are significantly disfavoured by the study of the WDLF. It is worth noting that the high mass of the axion derived in those works is a direct consequence of the identification of the 215 s (213 s) mode of G117-B15A (R548) as a mode trapped in the envelope. Consequently, our result can also be viewed as a strong argument that those modes are not trapped modes. This is true independent of the normalization of the theoretical WDLF. When comparing with the WDLF of [48] that includes information from an extended range of luminosities ($3 < M_{\rm Bol} < 12.5$) we find that values of $m_a \cos^2\beta \gtrsim 10$ meV are strongly at variance with the WDLF. In particular a χ^2-test suggests that values of $m_a \cos^2\beta \gtrsim 10$ meV are discarded at a 3σ confidence level. Unfortunately, it is not possible to attach a credible confidence level to all these results, as discrepancies between different observed WDLF, as well as a lack of a proper estimation of the uncertainties in the SFR, prevent us from doing so. It should be noted, however, that uncertainties in the theoretical WDLFs might not be dominant. In fact, numerical experiments suggest that possible fluctuations of the order of 50% in the SFR during the last 1.5 Gyr, as those suggested by [49], would only translate into an uncertainty of less than a 10% in the WDLF. In addition, current uncertainties in the cooling times of white dwarfs are below a 10% [40, 50] and would imply a similar uncertainty in the WDLF. Uncertainties of the order of 10% in the theoretical WDLF are not expected to affect significantly the constraints derived in section 4.2. On the other hand discrepancies between different observed WDLF are significant. Note, for example that, while the WDLF of [17] favours almost no extra cooling mechanism ($m_a \cos^2\beta \lesssim 2.5$ meV) axion masses below $m_a \cos^2\beta \simeq 10$ meV are not excluded by our current knowledge of the WDLF of the Galactic disk. In particular, it is worth noting that the features in some WDLFs [18, 20] can be interpreted as suggestions for axion masses in the range 2.5 meV$\lesssim m_a \cos^2\beta \lesssim 7.5$ meV. This is particularly interesting in the light of the forthcoming International Axion Observatory (IAXO, [51]) which will be able to explore axion masses in the range $m_a \cos^2\beta \gtrsim 3$ meV.

Needles to say, more work needs to be done. In particular completely independent WDLFs, like those presented by [19, 20, 52], are needed in order to account for possible systematics in the determinations. In particular, the new WDLFs being derived from the DR10-SDSS (Kepler, private communication), which will include a much larger range of WD luminosities will significantly improve our constraints. On the theoretical side a more complex approach (e.g. [53]) is needed to account for the theoretical uncertainties in the construction of the WDLF. In particular the impact of the uncertainties in the SFR, Galactic dynamics and the H-rich/H-deficient white dwarf ratio need to be assessed.

Acknowledgments

The authors thank H. Harris, S. DeGennaro, N. Rowell and N. Hambly for the data of their respective WDLF. We also thank G. Raffelt and A. Córsico for reading a preliminar version of the manuscript and making useful suggestions. This research was supported by PIP 112-200801-00940 from CONICET and through the Programa de Modernización Tecnológica of the ANPCYT, BID 1728/OC-AR. M3B is supported by a fellowship for postdoctoral researchers from the Alexander von Humboldt Foundation.

References

[1] R.D. Peccei and H.R. Quinn, *CP Conservation in the Presence of Instantons*, *Phys. Rev. Lett.* **38** (1977) 1440 [INSPIRE].

[2] F. Wilczek, *Problem of Strong p and t Invariance in the Presence of Instantons*, *Phys. Rev. Lett.* **40** (1978) 279 [INSPIRE].

[3] S. Weinberg, *A New Light Boson?*, *Phys. Rev. Lett.* **40** (1978) 223 [INSPIRE].

[4] M.I. Vysotsky, Y. Zeldovich, M.Y. Khlopov and V.M. Chechetkin, *Some Astrophysical Limitations on Axion Mass*, *Sov. JETP Lett.* **27** (1978) 502 [*Pisma Zh. Eksp. Teor. Fiz.* **27** (1978) 533] [INSPIRE].

[5] A.R. Zhitnitsky, *On Possible Suppression of the Axion Hadron Interactions. (In Russian)*, *Sov. J. Nucl. Phys.* **31** (1980) 260 [INSPIRE].

[6] M. Dine, W. Fischler and M. Srednicki, *A Simple Solution to the Strong CP Problem with a Harmless Axion*, *Phys. Lett.* **B 104** (1981) 199 [INSPIRE].

[7] J.E. Kim, *Weak Interaction Singlet and Strong CP Invariance*, *Phys. Rev. Lett.* **43** (1979) 103 [INSPIRE].

[8] M.A. Shifman, A.I. Vainshtein and V.I. Zakharov, *Can Confinement Ensure Natural CP Invariance of Strong Interactions?*, *Nucl. Phys.* **B 166** (1980) 493 [INSPIRE].

[9] G.G. Raffelt, *Stars as laboratories for fundamental physics*, University of Chicago Press (1996).

[10] G.G. Raffelt, *Axion Constraints From White Dwarf Cooling Times*, *Phys. Lett.* **B 166** (1986) 402 [INSPIRE].

[11] J. Isern, M. Hernanz and E. Garcia-Berro, *Axion cooling of white dwarfs*, *Astrophys. J.* **392** (1992) L23 [INSPIRE].

[12] J. Isern, E. Garcia-Berro, S. Torres and S. Catalan, *Axions and the cooling of white dwarf stars*, *Astrophys. J. Lett.* **682** (2008) 109 [arXiv:0806.2807] [INSPIRE].

[13] N. Viaux, M. Catelan, P.B. Stetson, G. Raffelt, J. Redondo et al., *Particle-physics constraints from the globular cluster M5: Neutrino Dipole Moments*, *Astron. Astrophys.* **558** (2013) A12 [arXiv:1308.4627] [INSPIRE].

[14] D.E. Winget, D.J. Sullivan, T.S. Metcalfe, S.D. Kawaler and M.H. Montgomery, *A strong test of electro-weak theory using pulsating db white dwarf stars as plasmon neutrino detectors*, *Astrophys. J.* **602** (2004) L109 [astro-ph/0312303] [INSPIRE].

[15] L.G. Althaus, A.H. Corsico, S. Torres, P. Loren-Aguilar, J. Isern et al., *The evolution of white dwarfs with a varying gravitational constant*, *Astron. Astrophys.* **527** (2011) 72 [arXiv:1101.0986] [INSPIRE].

[16] H.K. Dreiner, J.-F. Fortin, J. Isern and L. Ubaldi, *White Dwarfs constrain Dark Forces*, *Phys. Rev.* **D 88** (2013) 043517 [arXiv:1303.7232] [INSPIRE].

[17] H.C. Harris, J.A. Munn, M. Kilic, J. Liebert, K.A. Williams et al., *The white dwarf luminosity function from sdss imaging data*, *Astron. J.* **131** (2006) 571 [astro-ph/0510820] [INSPIRE].

[18] S. DeGennaro, T. von Hippel, D.E. Winget, S.O. Kepler, A. Nitta et al., *White Dwarf Luminosity and Mass Functions from Sloan Digital Sky Survey Spectra*, *Astron. J.* **135** (2008) 1 [arXiv:0709.2190] [INSPIRE].

[19] J. Krzesinski, S.J. Kleinman, A. Nitta, S. Hügelmeyer, S. Dreizler, J. Liebert et al., *A hot white dwarf luminosity function from the Sloan Digital Sky Survey*, *Astron. Astrophys.* **508** (2009) 339.

[20] N. Rowell and N.C. Hambly, *White dwarfs in the SuperCOSMOS Sky Survey: the thin disc, thick disc and spheroid luminosity functions*, *Mon. Not. Roy. Astron. Soc.* **417** (2011) 93.

[21] J. Isern and E. García-Berro, *White dwarfs as physics laboratories: the axion case.*, *Mem. Soc. Astron. Italiana* **79** (2008) 545.

[22] J. Isern, S. Catalan, E. Garcia-Berro and S. Torres, *Axions and the white dwarf luminosity function*, *J. Phys. Conf. Ser.* **172** (2009) 012005 [arXiv:0812.3043] [INSPIRE].

JCAP10(2014)069

[23] J. Isern, E. Garcia-Berro, L.G. Althaus and A.H. Corsico, *Axions and the pulsation periods of variable white dwarfs revisited*, *Astron. Astrophys.* **512** (2010) A86 [arXiv:1001.5248] [INSPIRE].

[24] A. Bischoff-Kim, M.H. Montgomery and D.E. Winget, *Strong limits on the DFSZ axion mass with G117-B15A*, *Astrophys. J.* **675** (2008) 1512 [arXiv:0711.2041] [INSPIRE].

[25] A.H. Corsico, L.G. Althaus, M.M.M. Bertolami, A.D. Romero, E. Garcia-Berro et al., *The rate of cooling of the pulsating white dwarf star G117-B15A: a new asteroseismological inference of the axion mass*, *Mon. Not. Roy. Astron. Soc.* **424** (2012) 2792 [arXiv:1205.6180] [INSPIRE].

[26] A.H. Corsico, L.G. Althaus, A.D. Romero, A.S. Mukadam, E. Garcia-Berro et al., *An independent limit on the axion mass from the variable white dwarf star R548*, *JCAP* **12** (2012) 010 [arXiv:1211.3389] [INSPIRE].

[27] S.O. Kepler, J.E.S. Costa, B.G. Castanheira, D.E. Winget, F. Mullally et al., *Measuring the evolution of the most stable optical clock g 117-b15a*, *Astrophys. J.* **634** (2005) 1311 [astro-ph/0507487] [INSPIRE].

[28] L.G. Althaus, A.M. Serenelli, J.A. Panei, A.H. Corsico, E. Garcia-Berro et al., *The Formation and evolution of hydrogen-deficient post-AGB white dwarfs: The Emerging chemical profile and the expectations for the PG1159-DB-DQ evolutionary connection*, *Astron. Astrophys.* **435** (2005) 631 [astro-ph/0502005] [INSPIRE].

[29] I. Renedo, L.G. Althaus, M.M.M. Bertolami, A.D. Romero, A.H. Corsico et al., *New cooling sequences for old white dwarfs*, *Astrophys. J.* **717** (2010) 183 [arXiv:1005.2170] [INSPIRE].

[30] M.M. Miller Bertolami, L.G. Althaus and E. Garcia-Berro, *Quiescent nuclear burning in low-metallicity white dwarfs*, *Astrophys. J.* **775** (2013) L22 [arXiv:1308.2062] [INSPIRE].

[31] L. Segretain, G. Chabrier, M. Hernanz, E. Garcia-Berro, J. Isern and R. Mochkovitch, *Cooling theory of crystallized white dwarfs*, *Astrophys. J.* **434** (1994) 641.

[32] G. Magni and I. Mazzitelli, *Thermodynamic properties and equations of state for hydrogen and helium in stellar conditions*, *Astron. Astrophys.* **72** (1979) 134.

[33] S. Cassisi, A.Y. Potekhin, A. Pietrinferni, M. Catelan and M. Salaris, *Updated Electron-Conduction Opacities: The Impact on Low-Mass Stellar Models*, *Astrophys. J.* **661** (2007) 1094 [astro-ph/0703011] [INSPIRE].

[34] C.A. Iglesias and F.J. Rogers, *Updated Opal Opacities*, *Astrophys. J.* **464** (1996) 943 [INSPIRE].

[35] J.W. Ferguson, D.R. Alexander, F. Allard, T. Barman, J.G. Bodnarik et al., *Low temperature opacities*, *Astrophys. J.* **623** (2005) 585 [astro-ph/0502045] [INSPIRE].

[36] R.D. Rohrmann, L.G. Althaus, E. Garcia-Berro, A.H. Corsico and M.M.M. Bertolami, *Outer boundary conditions for evolving cool white dwarfs*, *Astron. Astrophys.* **546** (2012) A119 [arXiv:1209.2452] [INSPIRE].

[37] N. Itoh, H. Hayashi, A. Nishikawa and Y. Kohyama, *Neutrino Energy Loss in Stellar Interiors. VII. Pair, Photo-, Plasma, Bremsstrahlung, and Recombination Neutrino Processes*, *Astrophys. J. Suppl.* **102** (1996) 411.

[38] M. Haft, G. Raffelt and A. Weiss, *Standard and nonstandard plasma neutrino emission revisited*, *Astrophys. J.* **425** (1994) 222 [*Erratum ibid.* **438** (1995) 1017] [astro-ph/9309014] [INSPIRE].

[39] J.M. Burgers, *Flow Equations for Composite Gases*, Academic Press, New York (1969).

[40] M. Salaris, L.G. Althaus and E. García-Berro, *Comparison of theoretical white dwarf cooling timescales*, *Astron. Astrophys.* **555** (2013) A96 [arXiv:1306.2575] [INSPIRE].

[41] A.D. Romero, *Astrosismología de estrellas enanas blancas variables ZZ Ceti*, Ph.D. Thesis, Universidad Nacional de La Plata (2012).

[42] M. Salaris, A. Serenelli, A. Weiss and M.M. Bertolami, *Semi-empirical white dwarf initial-final mass relationships: a thorough analysis of systematic uncertainties due to stellar evolution models*, *Astrophys. J.* **692** (2009) 1013 [arXiv:0807.3567] [INSPIRE].

[43] M. Nakagawa, Y. Kohyama and N. Itoh, *Axion Bremsstrahlung in Dense Stars*, *Astrophys. J.* **322** (1987) 291 [INSPIRE].

[44] M. Nakagawa, T. Adachi, Y. Kohyama and N. Itoh, *Axion bremsstrahlung in dense stars. II - Phonon contributions*, *Astrophys. J.* **326** (1988) 241.

[45] G. Raffelt and A. Weiss, *Red giant bound on the axion - electron coupling revisited*, *Phys. Rev.* **D 51** (1995) 1495 [hep-ph/9410205] [INSPIRE].

[46] I. Iben Jr. and G. Laughlin, *A study of the white dwarf luminosity function*, *Astrophys. J.* **341** (1989) 312.

[47] A. Pietrinferni, S. Cassisi, M. Salaris and F. Castelli, *A Large stellar evolution database for population synthesis studies. 1. Scaled solar models and isochrones*, *Astrophys. J.* **612** (2004) 168 [astro-ph/0405193] [INSPIRE].

[48] M.M. Miller Bertolami, *Limits on the neutrino magnetic dipole moment from the luminosity function of hot white dwarfs*, *Astron. Astrophys.* **562** (2014) A123.

[49] N. Rowell, *The Star Formation History of the Solar Neighbourhood from the White Dwarf Luminosity Function*, *Mon. Not. Roy. Astron. Soc.* **434** (2013) 1549 [arXiv:1306.4195] [INSPIRE].

[50] M. Salaris, S. Cassisi, A. Pietrinferni, P.M. Kowalski and J. Isern, *A large stellar evolution database for population synthesis studies: VI. White dwarf cooling sequences*, *Astrophys. J.* **716** (2010) 1241 [arXiv:1005.1791] [INSPIRE].

[51] J.K. Vogel, F.T. Avignone, G. Cantatore, J.M. Carmona, S. Caspi et al., *IAXO - The International Axion Observatory*, arXiv:1302.3273 [INSPIRE].

[52] S.O. Kepler, *Mass Distribution and Luminosity Functions for DAs and DBs*, in *18th European White Dwarf Workshop.*, J. Krzesiński, G. Stachowski, P. Moskalik and K. Bajan, eds., *Astron. Soc. Pacific Conf. Ser.* **469** (2013) 83.

[53] E.M. Geijo, S. Torres, J. Isern and E. Garcia-Berro, *The white dwarf luminosity function. I. Statistical errors and alternatives*, *Mon. Not. Roy. Astron. Soc.* **369** (2006) 1654 [astro-ph/0603612] [INSPIRE].